Effect of Channel Shape on Hall thruster Performance Using Argon and Xenon propellant

IEPC-2019-A563

Presented at the 36th International Electric Propulsion Conference
University of Vienna • Vienna • Austria
September 15 – 20, 2019

Junko Yamasaki[1], Shigeru Yokota[2], Kohei Shimamura[3]
University of Tsukuba, Tsukuba, Ibaraki, 305-8573, Japan

Abstract: Recently, alternative propellant is required because xenon price is increasing yearly. Argon which is the cheapest gas to use EPs, have not been a strong candidate because of its poor performance. Therefore we improved Hall thruster shape to enhance argon performance. We clarified that the shorter channel length is suitable for the xenon propellant, while the longer discharge channel is suitable for the argon propellant from the view point of thrust performance and longer lifetime.

Nomenclature

I_{sp}	=	specific impulse
η_t	=	anode efficiency
η_u	=	mass utilization efficiency
C_{total}	=	total transportation cost
C_{unit}	=	unit cost
$C_{insuarance}$	=	insurance cost
C_{launch}	=	launch cost
C_{prop}	=	propellant cost
$C_{operation}$	=	operation cost
D	=	depreciation expense
m_{f}	=	dry mass
m_{prop}	=	propellant mass
m_{body}	=	weight owithout the tank
M_{tank}	=	weight of the tank
β	=	safety factor
ρ	=	material density
R	=	gas constant
T	=	temperature
m	=	weight per mole
σ	=	breaking strength
α_1	=	propellant price per kg
α_2	=	personnel expenses per second
ΔV	=	speed increment
g	=	gravitational acceleration

[1] Student, Department of Engineering Mechanics and Energy, yamasaki@spl.kz.tsukuba.ac.jp
[2] Associate Professor, Division of Engineering Mechanics and Energy, yokota@kz.tsukuba.ac.jp
[3] Assistant Professor, Division of Engineering Mechanics and Energy, shimamura@kz.tsukuba.ac.jp

TF	=	tankage fraction
V_{LEO}	=	speed at LEO
$\Delta C_{\mathrm{launch}}$	=	launch cost per kg
V_{GEO}	=	speed at GEO
Δi	=	orbital inclination
Q	=	collision cross section, m^2
r	=	cylindrical coordinate component, m
z	=	cylindrical coordinate component, m
ε_0	=	permittivity of vacuum, F/m
θ	=	cylindrical coordinate component, rad
ϕ	=	potential, V
E	=	electric field, V/m
n	=	neutral particle
e	=	electron
i	=	ion

I. Introduction

Cost reduction of 11 million dollar is possible by using an electrical propulsion system instead of chemical propulsion system.[1)] However total cost reduction is limited by using expensive xenon as propellant. In addition, xenon is likely to exhaust in the future.[2)] Therefore, a lot of alternative propellants are researched actively all over the world (See Table.1). Solid propellant need evaporate system, krypton and argon have lower performance than xenon, only krypton was actually used for FM.[2, 3)] Low performance lead increase power supply mass and tank mass resulting in increased launch cost and longer orbit transition time leads to increase operation costs. However, the cost of changing the propellant has not been evaluated. While argon is appearing for an alternative propellant for Hall thrusters due to its low price, however it has not been a strong candidate because of its relatively poor performance, especially propellant utilization efficiency. [4)]

In order to use the argon propellant practically, it is necessary to clarify the trade-off relationship between the cost and the thrust performance. Thus, in our previous research, firstly, we had built a space transportation cost model and cleared that argon-xenon mixture propellant effective to improve the ionization of argon and consequently lower the transportation cost.[5)] Our objective in this paper is to report the results of simulations to optimize thrusters for argon and reveal the performance of modified Hall thruster. We also examined transportation cost in the case of geosynchronous orbit satellites and compared with using xenon optimized Hall thruster and modified for argon Hall thruster.

Table 1 Variable propellant performance.

Element	Xe[6)]	Ar[7)]	Kr[8)]	Bi[9)]	Mg[10)]	Zn[11)]
Atomic Mass	131.3	39.9	83.8	209.0	24.3	65.4
First Ionization Potential, eV	12.1	15.8	14	7.3	7.64	9.4
Cost, $/kg	5000	1.3	101	9	1.8	1.8
Discharge Voltage, V	300	250	250	-	300	250
Anode Efficiency, %	43.6	23.5	28.5	-	22	49
Specific Impulse, s	1483	1864	1200	-	2300	2104

II. Hall Thruster with longer discharge channel

Since argon has higher ionization potential than xenon, the thrust performance is worse than that of xenon in principle. On the other hand, depending on the thrust efficiency, argon propellant may be able to produce the higher

I_{sp} than xenon propellant because argon ions and neutrals exhaust velocities are much higher than those of xenon due to its lighter mass. [2)]

In general, Hall thrusters are designed to optimize for xenon, it is not suit for argon or other propellant. Therefore, we propose to redesign Hall thruster for argon propellant. As is mentioned above, due to argon ions and neutrals velocities are higher than that of xenon, it is necessary to increase the argon neutrals residence time within the channel to increase the chance to ionize. To expand the discharge area of argon, we redesigned longer discharge channel to widen the magnetic field.

Fig.1 shows the redesigned Hall thruster for argon propellant. While xenon optimized Hall thruster has 3 mm discharge channel length, the redesigned Hall thruster has 9 mm channel length. Figure 2 shows the radial magnetic field profiles calculated by a finite element method solver: FEMM. 3 mm channel and 9 mm channel. There is a peak exterior the exit plane with 3 mm channel, while with 9 mm channel, more gentle magnetic field distribution and the peak is inside the channel. Therefore, it is expected that potential distribution is gradually with 9 mm channel.

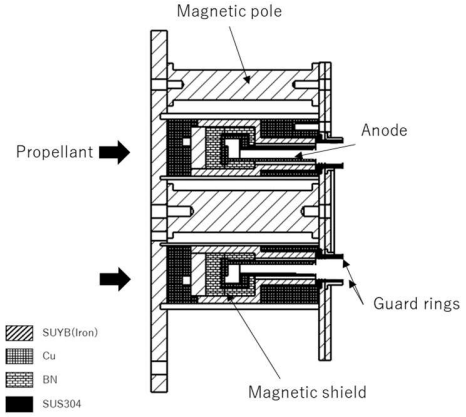

Fig. 1. Redesigned Hall thruster for argon.

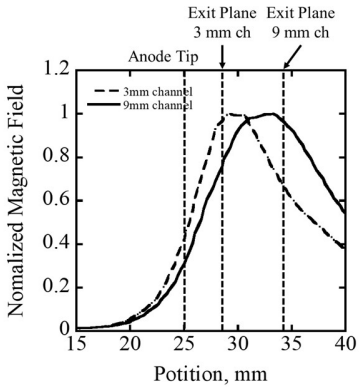

Fig. 2. Magnetic field distribution of 3 mm and 9 mm discharge channel.

III.Prediction by Numerical Simulation

To predict the effect of promoting ionization by channel length, particle-in-cell (PIC) simulation was used. We use (r, θ, z) cylindrical coordinates. The position component of the particle is represented by (r, z) and the velocity component is represented by (r, θ, z), that is, 2D3V. [14)] The calculation area is as shown in Figure 3, and the numbers of grid in the r and z axis direction are 30 and 60, respectively. Interparticle collisions are solved using the Direct simulation Monte Carlo (DSMC). In this program, only collisions of neutral particles and electrons e^- are considered. There are 3 types of collisions: primary ionization collision, primary excitation collision and elastic scattering. Other collisions are ignored because the collision frequency is smaller than these collisions due to the relationship between the number density and the relative velocity. Therefore, the total collision cross section Q_t is expressed by the Eq. (12).

$$Q_t = Q_{ion} + Q_{ex} + Q_{ela} \tag{12}$$

Although there is Bohm diffusion [15,16)] as one of the models of the electron anomalous diffusion, in order to evaluate whether or not the anomalous diffusion is reproduced by the electrostatic sheath, and for the influence on the electron orbit when it reproduced. For this reason, in this program, we didn't implement Bohm diffusion. The potential and electric field are obtained by solving Poisson's equation, Eq. (13) by the Successive Over-Relaxation (SOR) method and the electric field is obtained from the relationship between the potential in the electrostatic field and electric filed, Eq. (14).

$$\frac{\partial^2 \phi}{\partial z^2} + \frac{1}{r}\frac{\partial}{\partial r}\left(r\frac{\partial \phi}{\partial r}\right) = -\frac{e}{\varepsilon_0}(n_i - n_e) \tag{13}$$

$$\boldsymbol{E} = -\nabla\phi \tag{14}$$

We use the artificial electron mass to accelerate the calculation and the electron mass is 2500 times the actual one. By introducing the artificial electron mass, the Larmor radius becomes larger than the actual one and the collision

cross section becomes smaller than the actual one, so correction is made by multiplying the magnetic field acting on the electrons and the collision cross section by $\sqrt{2500}$ times.
In addition, we use Mersenne Twister as a random number for particle collision detection in DSMC and the period of this random number is $2^{19337} - 1$.

Figure 4 and 5 show electron density inside discharge channel on xenon propellant. Xenon is ionized more upstream than argon and ion density is not increased by longer channel. While, the ionization occurs in relatively downstream region in the argon case (see Figure 5); when using lighter gas as a propellant, the ionization region goes to downstream.

From these results, it is expected that ionization of argon will be promoted by using a longer channel.

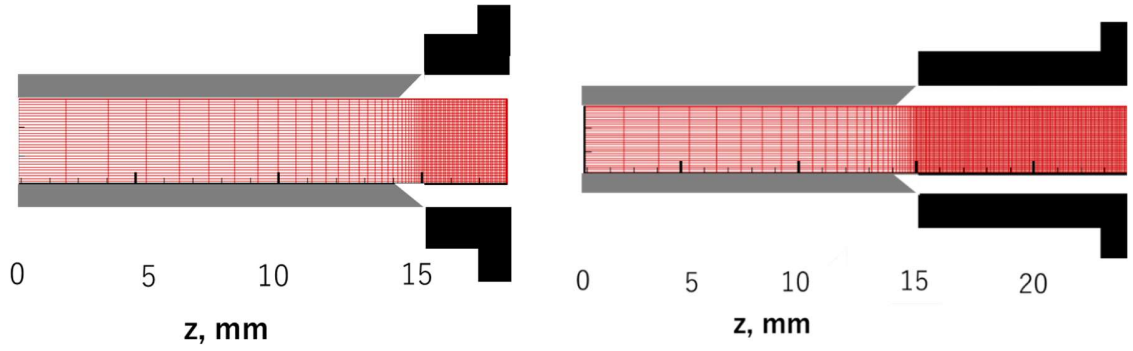

(A) Shorter channel (3mm) **(B) Longer channel(9mm)**

Figure.3 Calculation region.

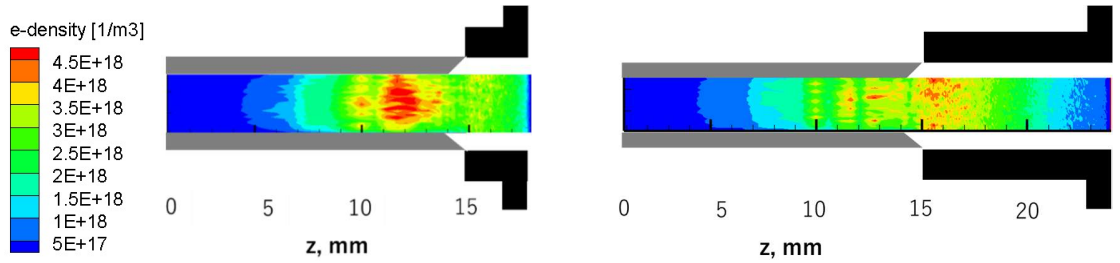

(A) Shorter channel (3mm) **(B) Longer channel(9mm)**

Figure 4. Electron density inside discharge channel on xenon propellant.

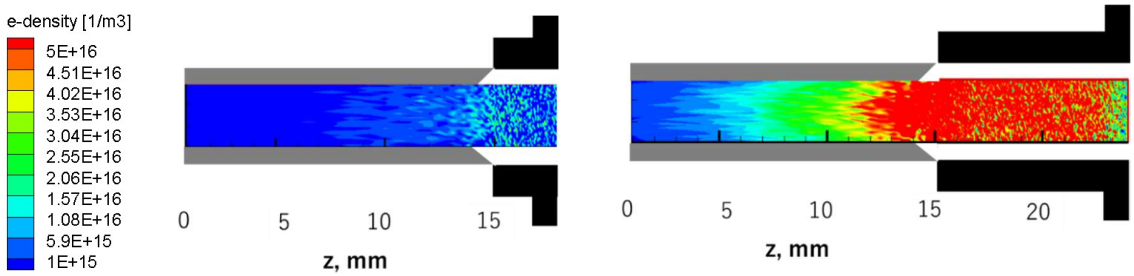

(A) Shorter channel (3mm) **(B) Longer channel(9mm)**

Figure 5. Electron density inside discharge channel on argon propellant.

IV.Experimental verification

Based on the above prediction, we redesigned 700W class 3 mm channel and 9 mm channel Hall thruster and verified by experiment.

Magnetic shield was installed around anode to prevent magnetic field applying in the anode by previous research. [17] For the propellant, xenon gas and argon gas with purity of 99.999% were used. For cathode Hollow Cathode was used and filament cathode was used for ignition. The Hall thruster was operated in a vacuum chamber whose diameter and length were both 1.0 m. The vacuum chamber was evacuated by a turbo molecular pump (3000 L/s) backed by a rotary pump (1500 L/min). The backpressure reached a maximum of 3.8×10^{-2} Pa in pure xenon, and a minimum of 2.6×10^{-2} Pa in pure argon.

Figure 6 shows schematic diagram of electric circuit. Discharge current was measured between power supply and anode with oscilloscope.

The thrust was measured using a pendulum type thrust stand that was used previously to evaluate various Hall thrusters. The mass flow rate was set at 2～5 $A_{eq.}$. The cathode propellant was 7～10 sccm of xenon. The discharge voltage was set at 200 V and 250 V. The magnetic flux density is arranged to maximize the thrust efficiency in each condition.

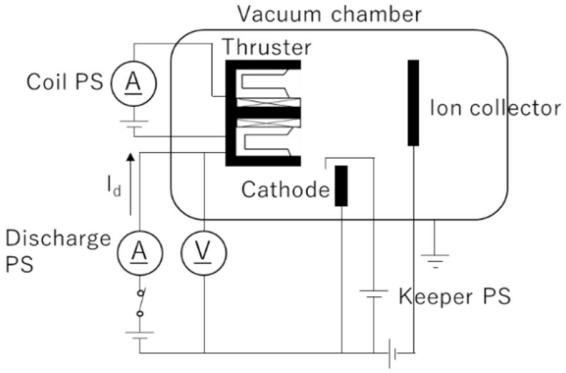

Figure 6. Electrical Circuit.

Figure 7 shows comparison of the anode efficiency and I_{sp}. As shown in these figures, I_{sp} in the case of mass flow rate 3Aeq, discharge voltage 250 V, increased from 973 s to 2227 s when using the extended channel on argon. This increment of I_{sp} is caused by the increase of the thrust efficiency; the thrust efficiency increased from 9 % to 22.3% using the extended channel. On the other hand, the I_{sp} of xenon were almost same or with and without extended channel in the case of mass flow rate 2 A_{eq}. However, the thrust efficiency with extended channel is 50 % less than that without extended channel. The possible scenario is as follows. Once ionized xenon collides with the discharge channel wall named guard rings and become a neutral atom. Before exhausted from the discharge channel the atom ionized again. It takes extra energy to ionize the xenon more than two times so that the thrust efficiency becomes lower. In addition, in the longer channel case, the data of more than 3 A_{eq} xenon and 4 A_{eq} argon weren't measured because of too high discharge current.

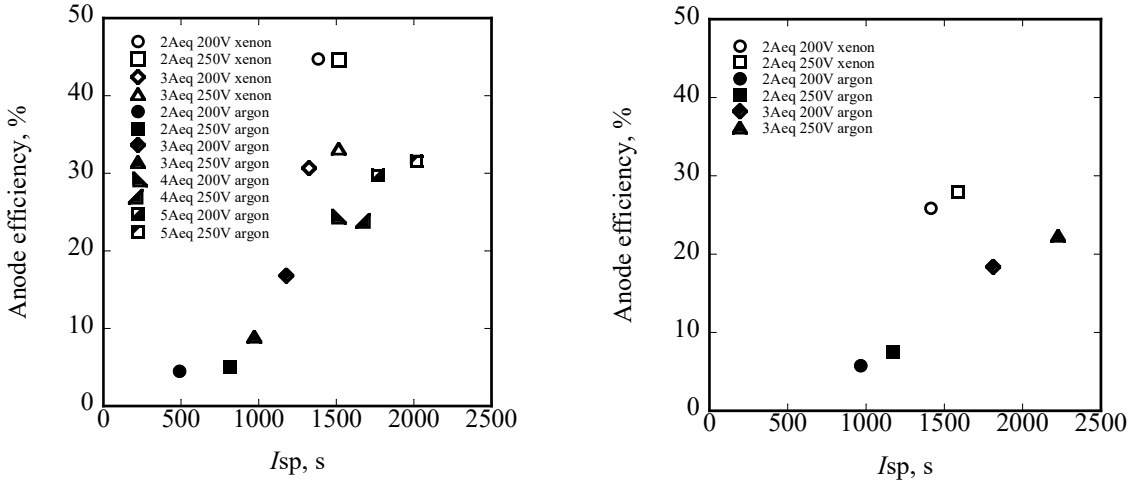

(A)Shorter channel (3mm) **(B)Longer channel(9mm)**

Figure 7. Comparison of thrust performance on argon and xenon.

V. Estimation by the cost

In this chapter, we introduce the cost model which was constructed in order to know the enough performance to reduce the cost using alternative propellant. The values are assumed to calculate the cost for lifecycle of mission in the case of geosynchronous orbit satellites.

The total spacecraft transportation cost is defined by K. Galabova et al. as following equation. [6)]

$$C_{\text{total}} = C_{\text{unit}} + C_{\text{insuarance}} + C_{\text{launch}} + C_{\text{prop}} + C_{\text{operation}} + D. \quad (1)$$

Here, C_{unit} , $C_{\text{insuarance}}$ and D are independent of performance of propulsion system, so that we ignore them. That is, we define the total cost is the sum of the costs for launch, propellant and operation.

$$C_{\text{total}} = C_{\text{launch}} + C_{\text{prop}} + C_{\text{operation}} \quad (2)$$

Here, C_{launch} is assumed to be proportional to the satellite wet mass. The launch cost is depending on the launch capability of rockets. When using Falcon9, ΔC_{launch} is 2.7 M$/ton.

$$C_{\text{launch}} = \Delta C_{\text{launch}}\left(m_{\text{prop}} + m_{\text{f}}\right) \quad (3)$$

The dry mass can be divided into the main body mass and the tank mass.

$$m_{\text{f}} = m_{\text{body}} + m_{\text{tank}} \quad (4)$$

The tank mass is calculated by using the following tankage fraction.

$$\text{TF} = \frac{m_{\text{tank}}}{m_{\text{prop}}} = \frac{3\beta\rho RT}{2m\sigma} \quad (5)$$

The tank weight ratios are 0.35 for argon and 0.08 for xenon in the case of using composite material. Liquid storage at cryogenic temperature is suggested for argon, and tankage fraction in that case is 0.04.[7)] In this case, a composite material is used for xenon (TF=0.08), and argon is stored at cryogenic temperature (TF=0.04).

Propellant costs are proportional to propellant mass.

$$C_{\text{prop}} = \alpha_1 m_{\text{prop}} \quad (6)$$

The propellant mass is calculated by Ziolkovsky equation.

$$m_{\text{prop}} = m_{\text{f}}\left[\exp\left(\Delta V / g\, I_{\text{sp}}\right) - 1\right] \quad (7)$$

The operation cost is a function of orbital transfer time. Transfer time was calculated using spiral transfer trajectory from LEO to GEO. It is important to consider cargo mission to take advantage of Hall thruster, first of all, we have estimated the case of geostationary satellite assuming the commercial satellite.

$$C_{\text{operation}} = \alpha_2 \Delta t \quad (8)$$

$$\Delta t = \frac{m_{\mathrm{prop}}}{\dot{m}} \tag{9}$$

$$\dot{m} = \frac{2\eta P}{g^2 I_{\mathrm{sp}}^2} \tag{10}$$

We used the value of Boeing 702SP bus specifications for m_{body} and ΔV. In the case of transfer from LEO to GEO by low acceleration thruster, ΔV is derived by Edelbaum.

$$\Delta V = \sqrt{V_{LEO}^2 - 2V_{LEO}V_{GEO}\cos\frac{\pi}{2}\Delta i + V_{GEO}^2} \tag{11}$$

Number of operators means number of people required for orbit transfer. The values of operators and personal expenses are from personal communications.

For example, assuming all electrified satellites, the cost was evaluated for alternative propellants in Table.1. Table 2 was used for the cost calculation conditions. Table 3 shows the cost comparison of xenon and argon propellant. Shorter channel is assumed to use for xenon and longer channel is assumed to use for argon. As shown in Table 3, transportation of argon propellant is 30% lower that xenon propellant for geostationary satellites.

Table 2 Values used for cost calculation.

Parameters	Value
$\alpha_{1\mathrm{Xe}}$, \$/kg	5000
$\alpha_{1\mathrm{Ar}}$, \$/kg	1.3
ΔV, m/s	2000
m_{body}, kg	2040
Number of operations	2
α_2, \$/hour	71
$\Delta C_{\mathrm{launch}}$, M\$/kg	2.7

Table 3. Cost comparison of xenon and argon propellant.

Propellant	xenon	argon
Channel	short	long
Propellant cost, M\$	0.00	5.41
Launch cost, M\$	9.5	8.1
Operation cost, M\$	3.14	1.19
Transportation cost, M\$	16.1	11.2

VI. Conclusion

The cost model to evaluate variable alternative propellant was built. Transportation cost is determined not only by thruster performance but also by tankage fraction or personal expense and so on. The result of cost estimation, transportation cost using xenon is 9.6 M\$ and that of argon is 22.7 M\$. Using improved thruster which is designed in University of Tsukuba, transportation cost using xenon is16.1 M\$ and that of argon is 11.2 M\$. From computational result, it is cleared that argon is ionized downstream, xenon is ionized upstream. Therefore longer channel is suitable for argon because widen magnetic field improve ionization of faster neutrals. While shorter channel is suitable xenon because it prevents the ions from hitting the wall.

Acknowledgments

This work was supported by JSPS KAKENHI Grant Number 19H02337 and 18H03815.

References

[1]K. Kinefuchi, N. Nagao, Y. Saito, K. Okita, K. Kuninaka. Test Facility Concept for High Power Electric Propulsion, STEP-2013-024, Space Transportation Symposium FY2013, 2014. (in Japanese)

[2]Eunsun Cha1, David B. Scharfe, Michelle K. Scharfe, and Mark A. Cappelli, Hybrid Simulations of Hall Thrusters Operating on Various Propellants. IEPC-2009-075, 29th International Electric Propulsion Conference, 2009.

[3]Richard R. Hofer et al. Factors Affecting the Efficiency of Krypton Hall Thrusters, 46th Meeting of the APS Division of Plasma Physics, 2004

[4]Daiki Fujita, "Operating parameters and oscillation characteristics of Anode-layer Hall thruster with argon propellant", ISTS paper 2013-s-07-b Soc. Aeronaut. Space Sci., 47 (2004), pp. 195–201.

[5]Junko Yamasaki, Shigeru Yokota, and Kohei Shimamura, Performance Enhancement of an Argon-Based Propellant in a Hall Thruster, vacuum, September 2018, in press.

[6]Kalina K. Galabova, Olivier L. de Weck, "Economic case for the retirement of geosynchronous communication satellites via space tugs", Acta Astronautica 58 (2006) pp.485 – 498.

[7]Bayers, D.C. Terdan, F.F, and Myers I.T., "Primary Electric Propulsion for Future Space Missions, " NASA TM 79141,MAY 1979.

[8]James J. Szabo," Characterization of a High Specific Impulse Xenon Hall Effect Thruster", 29th International Electric Propulsion Conference, IEPC-2005-324.

[9]Daiki Fujita, "Operating parameters and oscillation characteristics of Anode-layer Hall thruster with argon propellant", ISTS paper 2013-s-07-b Soc. Aeronaut. Space Sci., 47 (2004), pp. 195–201.

[10]Richard R. Hofer et al. Factors Affecting the Efficiency of Krypton Hall Thrusters, 46th Meeting of the APS Division of Plasma Physics, 2004

[11]Alex Kieckhafer, Lyon B. King, "Energetics of Propellant Options for High-Power Hall Thrusters", Proceedings of the Space Nuclear Conference 2005.

[12]Mark A. Hopkins, "EVALUATION OF MAGNESIUM AS A HALL THRUSTER PROPELLANT", P65-71.

[13] James J. Szabo," Light Metal Propellant Hall Thrusters", 31st International Electric Propulsion Conference.

[14]Masahiro Nonaka et al. "Numerical Simulation of TAL Type Hall Thruster", ISTS, 2019 to Examine Electron Transport Process

[15]Yokota, S., Hara, K., Cho, S., Takahashi, D., Komurasaki, K., and Arakawa, Y." The Difference between Anode Shapes in an Anode-layer Type Hall Thruster", Trans. Jpn. Soc. Aeronaut. Space Sci., 51(2003), pp.492–497.

[16]Ehedo, E., Martinez, C. P., and Gallardo, M. J." Characterization of the Plasma in a Hall Thruster", Proceedings of the 27st IEPC, Pasadena, USA, IEPC-01-17, 2001.

[17] Shigeru Yokota,Daisuke Takahashi, Shinatora Cho, Ryotaro Kaneko,Masaya Hosoda, Kimiya Komurasaki and Yoshihiro Arakawa : Magnetic Topology to Stabilize Ionization Oscillation in Anode-layer-type Hall Thruster, Transactions of the Japan Society for Aeronautical and Space Science, Aerospace Technology Japan, Vol.10, ists28, 2012.